Metal–Organic Frameworks

Deutsche Ausgabe: DOI: 10.1002/ange.201411202
Internationale Ausgabe: DOI: 10.1002/anie.201411202

The Direct Heat Measurement of Mechanical Energy Storage Metal–Organic Frameworks**

Julien Rodriguez, Isabelle Beurroies, Thierry Loiseau, Renaud Denoyel, and Philip L. Llewellyn**

Abstract: *In any process, the heat exchanged is an essential property required in its development. Whilst the work related to structural transitions of some flexible metal–organic frameworks (MOFs) has been quantified and linked with potential applications such as molecular springs or shock absorbers, the heat related to such transitions has never been directly measured. This has now been carried out with MIL-53(Al) using specifically devised calorimetry experiments. We project the importance of these heats in devices such as molecular springs or dampers.*

Metal–organic framework (MOF) materials are at the center of many research activities, which is due to their potential applications in many fields such as gas storage, separation of fluids, drug delivery, and catalysis.[1–4] Recently, another area has been proposed where the mechanical properties of flexible MOFs can be used in energy-related applications such as dampers (partial dissipation of mechanical energy), shock absorbers (total dissipation), or springs (no dissipation).[5–7]

Indeed, some MOFs can be found in various structural forms, depending on external conditions, that differ both by their pore size and their apparent (bulk) density. Whilst the term of flexibility is often used to describe this phenomenon, the transition from one structure to the other is most often non-continuous. Indeed, in many cases this resembles a first-order phase transition accompanied by hysteresis.

The change in porosity (that is, pore size and shape) has important consequences on the potential applications of such materials.[8–11] This was first followed in the area of adsorption, where increasing concentrations of gases or liquids inside the pores lead to structural transitions. Such transitions have been labeled as gate opening[12] or breathing.[8] In such systems, even though calorimetric measurements have been carried out, it is impossible to deconvolute the heats that are due to host–guest interactions and those due to the host framework transition.

Subsequently, similar structural transitions have been provoked with physical stimuli such as temperature[13] or external pressure.[5] With the latter, an isostatic pressure is imposed around the MOF with a non-wetting transmission fluid. The simplest means to carry out such experiments is to use mercury, which allows the system volume to be followed as a function of pressure (P). This approach was first demonstrated with MIL-53(Cr)[5] and successfully extended to MIL-53(Al),[7] MIL-53(In)-NH_2,[14] and MIL-47(V).[6] It is possible to calculate the density and volume variation (dV) of the material during the phase transition. This therefore allows an estimation of the work ($W = P\,\mathrm{d}V$) needed to overcome the energetic barrier between what is known as the large pore (LP) and narrow pore (NP) forms of these MOFs. Such experiments highlight that it is possible, by using a liquid that does not penetrate the pores for either size or wettability reasons, to perform cycles of closing/opening of the structure under the influence of external pressure. It is then possible to use flexible MOFs in mechanical energy storage type applications in a far simpler manner than previously suggested with non-wetting porous materials. The latter systems, where the process is intrusion/extrusion of liquids from the pores,[15,16] have been proposed as dampers for vehicle suspensions.[17]

Mechanical systems can be classified as either shock absorbers (irreversible compression), dampers (compression–decompression with hysteresis), or molecular springs (compression–decompression without hysteresis).[18] For any application, mercury cannot be retained as a pressure transmission fluid for safety reasons, and alternative fluids have already been proposed including silicon oil,[6] mineral oil,[14,19] fluorinert,[20] and 2-propanol.[21] Here, silicon oil was used to perform the compression–depression cycles with the sample placed inside a calorimeter. This allows a direct measurement of the heat evolved and thus, for the first time to our knowledge, to an estimation of the internal energy variation during the structural transition independently from the presence of hysteresis. This internal energy variation may then be compared to theoretical calculations. Another important application of the determination of compression–decompression heat is the prediction of the thermal behavior of such systems if introduced for example in dampers. The question indeed arises regarding the sensitivity of these new systems to temperature, namely, is the compression transition sensitive to temperature? If yes, the question of the evacuation of heat when the system undergoing fast cycles of pression–decompression has to be considered.

[*] Dr. J. Rodriguez, Dr. I. Beurroies, Dr. R. Denoyel, Dr. P. L. Llewellyn
Aix-Marseille University, CNRS, MADIREL (UMR 7246)
Centre Scientifique de St. Jérôme
13397 Marseille cedex 20 (France)
E-mail: isabelle.beurroies@univ-amu.fr
philip.llewellyn@univ-amu.fr
Homepage: http://madirel.univ-amu.fr
Dr. T. Loiseau
Unité de Catalyse et Chimie du Solide (UCCS)—UMR CNRS 8181,
Université de Lille Nord de France
59652 Villeneuve d'Ascq (France)

[**] We would like to thank the ANR "MODS" (ANR-12-BS10-0005) for funding and support of this project, and Dr. Christian Serre for fruitful discussions.

The present study was carried out with MIL-53(Al), which is built from $AlO_4(OH)_2$ octahedra interconnected by terephthalate ligands (oxy groups of the octahedra),[22] resulting in one-dimensional pores with a diamond shape and the unit cell variation from about 1400 $Å^3$ to 1000 $Å^3$. At room temperature and pressure, it is found in a large pore (LP) form with a channel opening of 7–8 Å in width. As in the case of MIL-53(Cr),[5] the sample was first studied by mercury porosimetry. Figure 1 shows the volume–pressure curve

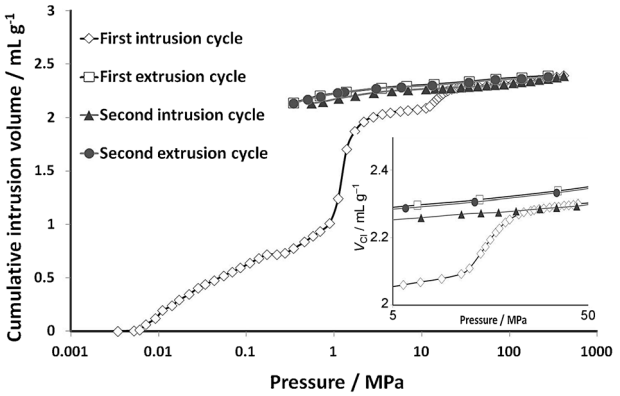

Figure 1. Cumulative volume of intruded mercury in two intrusion–extrusion cycles as a function of the applied pressure obtained for the MIL-53(Al) sample (inset: zoom between 5 and 50 MPa).

obtained with the MIL-53(Al) where three domains are observed along the intrusion curve. This curve compares well to a recent study.[7] Up to 1 MPa, the gradual intruded volume corresponds to the packing of the particle bed under mercury pressure.[23] Between 1 and 3 MPa, the volume step corresponds to the intrusion of mercury between particles. The second step which occurs at around 20 MPa, can only be interpreted by the transition from the LP to the NP phase, as 1) such material does not contain mesopores, based on nitrogen adsorption–desorption isotherm,[24] and 2) mercury cannot penetrate inside micropores. Furthermore, structural studies with other systems confirm such a transition with pressure.[6,14]

This compression step occurs at a pressure which is smaller than that observed either for MIL-53(Cr) (around 55 MPa[4]) or MIL-47(V) (around 85 MPa).[5] The volume variation during this step (0.24 mL g^{-1}) is comparable to that calculated from structure parameters obtained by XRD of approximately 0.3 mL g^{-1} (calculated from a volume variation of 29% from LP to NP and a density of 0.98 g mL^{-1} for LP form).[22,24] Contrary to the two other samples, the compression of MIL-53(Al) is not reversible in the analyzed pressure range: after decreasing the pressure, the LP form is not fully recovered. Indeed, in previous work the authors suggested that this sample could be used as a shock absorber.[7]

Figure 2 shows the same type of experiment that was carried out with silicon oil (see description of the procedure in the Experimental Section). Figure 3 shows the heat dissipated during the experiment. All of these data are corrected for the compressibility of the oil. As for the mercury experiment,

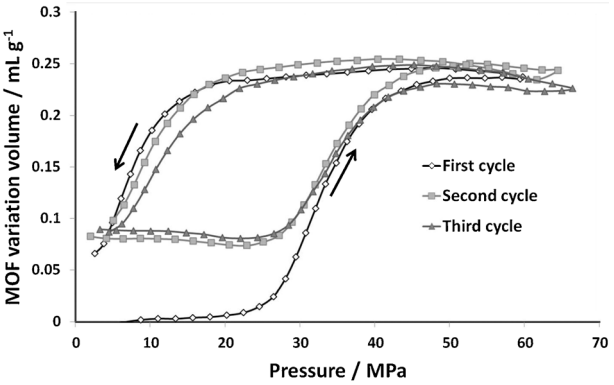

Figure 2. MOF volume variation as a function of the applied oil pressure on the MIL-53(Al) sample in three cycles of compression–decompression.

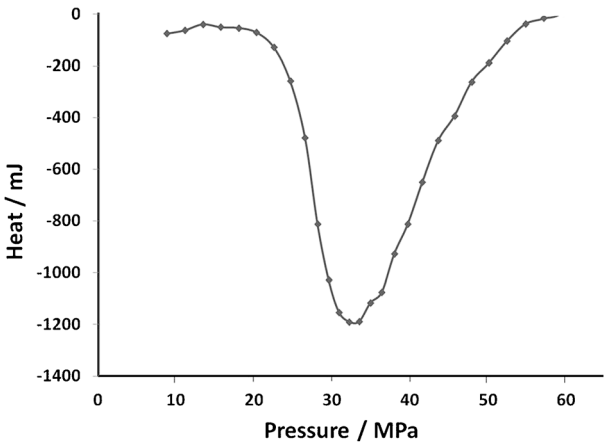

Figure 3. Compression heat as a function of the applied oil pressure on the MIL-53(Al) sample.

there is a step in the pressure/volume curve in Figure 2 that can be interpreted by the transition from large to narrow pore form. Contrary to the experiment with mercury, there is no step corresponding to interparticle penetration as the silicone oil is a wetting fluid that can spontaneously occupy the interparticle domain. However, the molecules are purportedly too bulky to penetrate into the MOF micropores. Several observations can be made: 1) several cycles of compression–decompression can be carried out successively; 2) there is a hysteresis, but the phenomenon is reversible after the first cycle; and 3) there is a partial loss of compression volume after the first compression, but the first decompression and the following cycles can be superimposed, within experimental error. It thus seems possible than a part of the long chain constituting the silicone oil could partially penetrate into some pores (perhaps the openings) and therefore be responsible of the difference after the first compression. However, this result clearly shows that silicon oil can be used as a fluid transmitter for such type of measurement and it can also be a good candidate for practical energy storage systems. Interestingly, in contrast to mercury, the MIL-53(Al)/silicon oil system shows the behavior of a damper.

Quantitatively, there are some differences between experiments with oil and mercury. Whereas the volume variation is similar for the first compression step (0.23 and 0.24 mL g^{-1} for oil and mercury respectively), the pressures corresponding to the transition steps for closing or opening the structure are different for the two experiments (Figure 4).

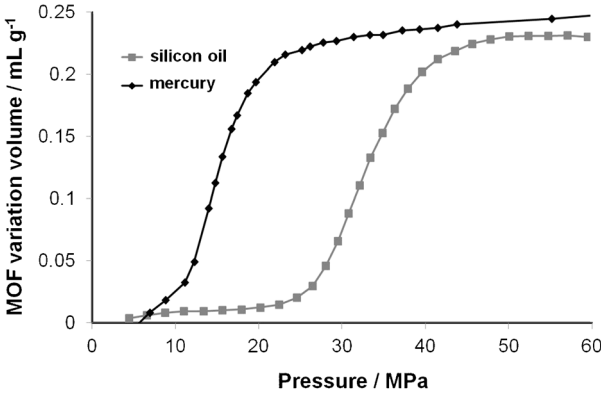

Figure 4. MOF volume variation as a function of the applied pressure of mercury and oil on the MIL-53(Al) sample during the first compression.

The pressures corresponding to the transitions are higher for oil than for mercury: 33 MPa versus 15 MPa at closing, and 7 MPa versus a pressure below 0.3 MPa at re-opening. Indeed, similar behavior was previously observed for the MIL-47(V) sample[5] although not discussed: the transition with mercury occurs at around 85 MPa whereas the transition with the same silicone oil is observed by XRD at 145 MPa. This difference in transition pressure, which depends on the liquid used for creating the isostatic pressure, may be the indication that the silicone oil partially penetrates at the entrance of the pores, as suggested above. Indeed, despite its high molecular weight and size ($Me_3SiO(SiMePhO)_x$-$(SiMe_2O)_ySiMe_3$), the size of the chain ends is of the same order as that of the pores.

Consequently, extra work may be needed to close the structure if the expulsion of this end of chain is required, whereas the reopening can occur at a higher pressure owing to the interaction between chain ends and pores entrances. This interpretation can be verified by using other types of oil. Nevertheless, the pressure range observed here for the MIL-53(Al)/silicon oil system (transition at around 33 MPa) is in the range required for vehicle shock absorbers (30–60 MPa).[17]

The full thermodynamic analysis of the data can be accomplished thanks to the simultaneous determination of heat during the compression/decompression cycles. It can be observed that the closing of the structure is exothermic (Figure 3), whereas the reopening is endothermic.

The internal energy (U) of the system can then be considered. The heat (Q) and work (W) produced during the closing, going from point A to point B in Figure 2, are obtained along an irreversible path, and a state function is needed to calculate the difference in energy between the LP and NP forms. Applying the first principle where the change in internal energy U is given by $\Delta U = Q + W$, it is possible to calculate this transition energy. The work W provided to the system is obtained from the $P = f(V)$ data (Figure 2) by integration between points A and B:

$$W = -\int_{A}^{B} P\,dV \qquad (1)$$

whereas the heat produced between A and B is calculated from the sum of heats at each pressure step (Figure 3). The resulting data are given in Table 1. Results are reported with regard to the mass of MOF.

Table 1: Experimental energy data of compression–decompression cycles for the MIL-53(Al) sample.

	Work [J g^{-1}]	Heat [J g^{-1}]	Internal energy [J g^{-1}]
cycle 1: Compression	7.8	−10.8	−3.0
cycle 1: decompression	−1.0	2.0	1.0
cycle 2: compression	7.0	−7.9	−0.9
cycle 2: decompression	−1.1	2.1	1.0
cycle 3: compression	6.0	−6.7	−0.7
cycle 3: decompression	−1.4	2.0	0.6

Interestingly, the heat is in the same order of magnitude as the work for all cycles, resulting in small internal energy variations (from −3.0 to 1.0 J g^{-1}). Indeed, if the mechanical work obtained for the first transition from large pore to narrow pore is about 7.8 J g^{-1}, the internal energy is significantly lower at −3.0 J g^{-1}. This result clearly shows that the thermal energy during compression–decompression cycles represents a non-negligible part and that the MIL-53(Al) structural transition could be sensitive to temperature. Thus, heat evacuation may need to be considered when using this material as a damper. Indeed, as shown in Table 1 after the first cycle, the heating is around −5 to −6 J g^{-1} $cycle^{-1}$. Without heat evacuation, this may lead to an increase in temperature of around 1 °C $cycle^{-1}$. In comparison, magneto-rheological fluid dampers often used in vehicles may heat from 20 to 100 °C during long working periods and large piston velocities, which may result in the loss of fluid stability and component failure.[30] In another example, with a hydro-pneumatic suspension combining a spring and damper into one unit, Els et al.[31] showed that the effect of the rise in gas temperature from 23 to 68 °C increased the spring oscillation rate by 58 % and the static ride height by 15 %. This all shows the heat measurement is a primary factor to determine the complete energetic profile of the system.

The data obtained here can be compared with data obtained from theoretical calculations and from indirect experiments. Theoretical calculations, based on the thermodynamic potentials in an osmotic ensemble have been applied

to gas–MOF systems to deconvolute the terms owing to host–guest interactions and host framework transition.[25,26] Here a free energy difference between the different LP and NP forms of MIL-53 of around $-7.5\ kJ\ mol^{-1}$ were obtained.

The direct calculations of the variation of internal energy obtained in this study can be further compared to other experimental estimations made during the MIL-53 structural transition. In most other approaches, the energy of transition is deduced of experiments where another process than the simple transition is present. For example, based on DSC experiments where drying of MIL-53(Cr) is analyzed, a value of −20 kJ per unit cell was deduced for the transition energy by considering the breathing MIL-53(Cr) and non-breathing MIL-53(Fe).[27] Other experiments of adsorption calorimetry[8,9] were carried out where the transition is present which give overall energies owing to host–guest interactions and framework transition. Interestingly, here in the case of CO_2 adsorption onto MIL-53(Al or Cr), two main regimes can be distinguished: at low pressure, closing is first observed followed by a second regime where reopening occurs. Looking in detail to this data, an exothermic peak is observed in the first regime (LP→NP) and an endothermic peak in the second regime (NP→LP), in agreement with trends observed in this study.

Concerning the application for mechanical energy storage, the preparation procedure of an oil/MOF system is simpler than that of systems based on hydrophobic porous materials, in general modified silica[16] or hydrophobic silicalite.[15] Moreover, as such there are no aging problems encountered so far with the MOF/oil system at this stage of the study, contrary to what is observed with silica in the presence of water.[17] However, more tests over a longer time period need to be performed to confirm this observation. In Table 2, the mechanical energy stored is compared for various systems. These are calculated by multiplying the transition pressure by the corresponding volume variation. The dissipated energy is calculated by integration of the work along the hysteresis loop. It can be observed that concerning both the stored energy and dissipated energy, MOFs outperform hydrophobic silica in many cases. Nonetheless, no MOF sample has shown the behavior of a spring until now (that is, with zero dissipated energy).

In future work, both device durability and resonance tests should be considered. Indeed, it should be borne in mind that a vehicle damper has a durability of around 10^6–10^7 cycles[17] and that the major vehicular structural resonances are in the frequency range from 0.1 to 100 Hz.[28] With the MOF/silicon oil system, resonance aging tests would allow both the overall heating and the ageing profile of this system to be established and could be compared with those obtained with other colloidal devices, such as hydrophobic silica/water systems.[29]

Experimental Section

The sample was weighed into a high-pressure cell and heated under vacuum to evacuate residual adsorbed molecules such as water such to obtain the LP (large pore) form of the material. The cell was then filled with silicone oil ($Me_3SiO(SiMePhO)_x(SiMe_2O)_ySiMe_3$) in a glove box under argon. The cell was then placed in the calorimetric cell and connected to the syringe pump by a manifold and the system was again evacuated with a primary pump. The syringe pump was filled with water. After thermal equilibrium, the valve between syringe pump and calorimetric cell containing sample and oil was opened. The syringe pushes water until contact with the silicone oil up to 0.2 MPa pressure. Water is insoluble in this oil and the density of oil is higher than that of water. The pressure was then increased in the cell step by step by injection of small volumes of water in the system (around 40 μL at each step). The sample volume, the equilibrium pressure, and the heat evolved are measured at each step. A blank experiment was carried out without sample to subtract from the raw data the variations of volume of water and oil that are due to their compressibilities as well as their heat of compression.

For mercury intrusion experiments, the sample is treated at 180 °C in situ in the penetrometer under primary vacuum and then sealed with grease such that the contact with air is as short as possible. The experiment was then carried out by first activating the sample down to 6.6 Pa and then introducing mercury is step by step up to 400 MPa.

Keywords: calorimetry · heat determination · mechanical properties · metal–organic frameworks · molecular springs

How to cite: *Angew. Chem. Int. Ed.* **2015**, *54*, 4626–4630
Angew. Chem. **2015**, *127*, 4709–4713

[1] G. Férey, *Chem. Soc. Rev.* **2008**, *37*, 191–214.
[2] G. Férey, C. Serre, T. Devic, G. Maurin, H. Jobic, P. L. Llewellyn, G. De Weireld, A. Vimont, M. Daturi, J. S. Chang, *Chem. Soc. Rev.* **2011**, *40*, 550–562.
[3] D. M. D'Alessandro, B. Smit, J. R. Long, *Angew. Chem. Int. Ed.* **2010**, *49*, 6058–6082; *Angew. Chem.* **2010**, *122*, 6194–6219.

Table 2: Characteristics of compression–decompression and water intrusion–extrusion for different matrices.

	P_{comp} [MPa]	P_{dec} [MPa]	Volume variation [$mL\,g^{-1}$]	W_{stored} [$J\,g^{-1}$]	W_{diss} [$J\,g^{-1}$]	Ref.
compression–decompression						
MIL-53(Al)[a]	33	7	0.23	7.7	5.9	this work
MIL-53(Al)[b]	15	0	0.24	6.6	6.6	[7]
MIL-47(V)[b]	85	60	0.3	33	10	[6]
MIL-53(Cr)[b]	55	10	0.25	13.75	11.25	[5]
water intrusion–extrusion						
ZIF-8	27	22	0.5	13.3	2.1	[32]
silicalite-1	96	91	0.11	11	0.7	[33]
pure silica ITQ-12 (ITW) zeolite	172	172	0.05	8.1	0	[34]
pure silica ITQ-4 (IFR) zeolite	42	0	0.14	5.7	5.7	[35]

[a] Compression with silicon oil. [b] Compression with mercury.

[4] P. Horcajada, C. Serre, M. Vallet-Regi, M. Sebban, F. Taulelle, G. Férey, *Angew. Chem. Int. Ed.* **2006**, *45*, 5974 – 5978; *Angew. Chem.* **2006**, *118*, 6120 – 6124.
[5] I. Beurroies, M. Boulhout, P. L. Llewellyn, B. Kuchta, G. Férey, C. Serre, R. Denoyel, *Angew. Chem. Int. Ed.* **2010**, *49*, 7526 – 7529; *Angew. Chem.* **2010**, *122*, 7688 – 7691.
[6] P. G. Yot, Q. Ma, J. Haines, Q. Yang, A. Ghoufi, T. Devic, C. Serre, V. Dmitriec, G. Férey, C. Zhong, G. Maurin, *Chem. Sci.* **2012**, *3*, 1100 – 1104.
[7] P. G. Yot, Z. Boudene, J. Macia, D. Granier, L. Vanduyfhuys, T. Verstraelen, V. Van Speybroeck, T. Devic, C. Serre, G. Férey, N. Stock, G. Maurin, *Chem. Commun.* **2014**, *50*, 9462 – 9464.
[8] S. Bourrelly, P. L. Llewellyn, C. Serre, F. Millange, T. Loiseau, G. Férey, *J. Am. Chem. Soc.* **2005**, *127*, 13519 – 13521.
[9] P. L. Llewellyn, G. Maurin, T. Devic, S. Loera-Serna, N. Rosenbach, C. Serre, S. Bourrelly, P. Horcajada, Y. Filinchuk, G. Férey, *J. Am. Chem. Soc.* **2008**, *130*, 12808 – 12814.
[10] L. Hamon, P. L. Llewellyn, T. Devic, A. Ghoufi, G. Clet, V. Guillerm, G. D. Pirngruber, G. Maurin, C. Serre, G. Driver, W. van Beek, E. Jolimaitre, A. Vimont, M. Daturi, G. Férey, *J. Am. Chem. Soc.* **2009**, *131*, 17490 – 17499.
[11] P. Horcajada, C. Serre, G. Maurin, N. A. Ramsahye, F. Balas, M. Vallet-Regi, M. Sebban, F. Taulelle, G. Férey, *J. Am. Chem. Soc.* **2008**, *130*, 6774 – 6780.
[12] T. Chokbunpiam, R. Chanajaree, T. Remsungnen, O. Saengsawang, S. Fritzsche, C. Chmelik, J. Caro, W. Janke, S. Hannongbua, *Microporous Mesoporous Mater.* **2014**, *187*, 1 – 6.
[13] Y. Liu, J.-H. Her, A. Dailly, J. Ramirez-Cuesta, D. A. Neumann, C. M. Brown, *J. Am. Chem. Soc.* **2008**, *130*, 11813 – 11818.
[14] P. Serra-Crespo, A. Dikhtiarenko, E. Stavitski, J. Juan-Alcañiz, F. Kapteijn, F.-X. Coudert, J. Gascon, *CrystEngComm* **2015**, *17*, 276 – 280.
[15] V. Eroshenko, R. C. Regis, M. Soulard, J. Patarin, *C. R. Phys.* **2002**, *3*, 111 – 119.
[16] Ya. Grosu, O. Ievtushenko, V. Eroshenko, J. M. Nedelec, J. P. E. Grolier, *Colloids Surf. A* **2014**, *441*, 549 – 555.
[17] C. V. Suciu, K. Yaguchi, *Exp. Mech.* **2009**, *49*, 383 – 393.
[18] B. Lefevre, A. Saugey, J. L. Barrat, L. Bocquet, E. Charlaix, P. F. Gobin, G. Vigier, *Colloids Surf. A* **2004**, *241*, 265 – 272.
[19] P. Serra-Crespo, E. Stavitski, F. Kapteijn, J. Gascon, *RSC Adv.* **2012**, *2*, 5051 – 5053.
[20] K. W. Chapman, G. J. Halder, P. J. Chapus, *J. Am. Chem. Soc.* **2009**, *131*, 17546 – 17547.
[21] E. C. Spencer, R. J. Angel, N. L. Ross, B. E. Hanson, J. A. K. Howard, *J. Am. Chem. Soc.* **2009**, *131*, 4022 – 4026.
[22] T. Loiseau, C. Serre, C. Huguenard, G. Fink, F. Taulelle, M. Henry, T. Bataille, G. Férey, *Chem. Eur. J.* **2004**, *10*, 1373 – 1382.
[23] H. Giesche, *Part. Part. Syst. Charact.* **2006**, *23*, 9 – 19.
[24] C. Serre, F. Millange, C. Thouvenot, M. Noguès, G. Marsolier, D. Louër, G. Férey, *J. Am. Chem. Soc.* **2002**, *124*, 13519 – 13526.
[25] F.-X. Coudert, M. Jeffroy, A. H. Fuchs, A. Boutin, C. Mellot-Draznieks, *J. Am. Chem. Soc.* **2008**, *130*, 14294 – 14302.
[26] D. Bousquet, F.-X. Coudert, A. Boutin, *J. Chem. Phys.* **2012**, *137*, 044118.
[27] S. Devautour-Vinot, G. Maurin, F. Henn, C. Serre, T. Devic, G. Férey, *Chem. Commun.* **2009**, 2733 – 2735.
[28] S. K. Jha, *J. Sound Vibration* **1976**, *47*, 543 – 558.
[29] C. V. Suciu, T. Iwatsubo, S. Deki, *J. Colloid Interface Sci.* **2003**, *259*, 62 – 80.
[30] M. B. Dogruoz, E. L. Wang, F. Gordaninejad, A. J. Stipanovic, *J. Intell. Mater. Syst. Struct.* **2003**, *14*, 79 – 86.
[31] P. S. Els, B. Grobbelaar, *J. Terramechanics* **1999**, *36*, 197 – 205.
[32] G. Ortiz, H. Nouali, C. Marichal, G. Chaplais, J. Patarin, *Phys. Chem. Chem. Phys.* **2013**, *15*, 4888 – 4891.
[33] L. Tzanis, H. Nouali, T. J. Daou, M. Soulard, J. Patarin, *Mater. Lett.* **2014**, *115*, 229 – 232.
[34] I. Khay, L. Tzanis, T. J. Daou, H. Nouali, A. Ryzhikov, J. Patarin, *Phys. Chem. Chem. Phys.* **2013**, *15*, 20320 – 20325.
[35] M. A. Saada, S. Rigolet, J.-L. Paillaud, N. Bats, M. Soulard, J. Patarin, *J. Phys. Chem. C* **2010**, *114*, 11650 – 11658.

Received: November 19, 2014
Revised: January 9, 2015
Published online: February 16, 2015

